Spreading dilatation in rat mesenteric arteries associated with calcium-independent endothelial cell hyperpolarization

Hiromichi Takano, Kim A. Dora, Michaela M. Spitaler and Chris J. Garland

Department of Pharmacy and Pharmacology, University of Bath, Bath BA2 7AY, UK

Both ACh and levcromakalim evoke smooth muscle cell hyperpolarization and associated relaxation in rat mesenteric resistance arteries. We investigated if they could evoke conducted vasodilatation along isolated arteries, whether this reflected spreading hyperpolarization and the possible mechanism involved. Focal micropipette application of either ACh, to stimulate endothelial cell muscarinic receptors, or levcromakalim, to activate smooth muscle K_{ATP} channels, each evoked a local dilatation (88 ± 14%, $n = 6$ and 92 ± 6% reversal of phenylephrine-induced tone, $n = 11$, respectively) that rapidly spread upstream (at 1.5 mm 46 ± 19%, $n = 6$ and 57 ± 13%, $n = 9$) to dilate the entire isolated artery. The local dilatation to ACh was associated with a rise in endothelial cell $[Ca^{2+}]_i$ ($F/F_{t=0} = 1.22 \pm 0.33$, $n = 14$) which did not spread beyond 0.5 mm ($F/F_{t=0} = 1.01 \pm 0.01$, $n = 14$), while the local dilatation to levcromakalim was not associated with any change in endothelial cell $[Ca^{2+}]_i$. In contrast, ACh and levcromakalim both stimulated local (12.7 ± 1.2 mV, $n = 10$ and 13.5 ± 4.7 mV, $n = 10$) and spreading (at 2 mm: 3.0 ± 1.1 mV, $n = 5$ and 4.1 ± 0.7 mV, $n = 5$) smooth muscle hyperpolarization. The spread of hyperpolarization could be prevented by cutting the artery, so was not due to a diffusible agent. Both the spreading dilatation and hyperpolarization were endothelium dependent. The injection of propidium iodide into either endothelial or smooth muscle cells revealed extensive dye coupling between the endothelial cells, but limited coupling between the smooth muscle cells. Some evidence for heterocellular spread of dye was also evident. Together, these data show that vasodilatation can spread over significant distances in mesenteric resistance arteries, and suggest this reflects an effective coupling between the endothelial cells to facilitate $[Ca^{2+}]_i$-independent spread of hyperpolarization.

(Received 24 December 2003; accepted after revision 13 February 2004; first published online 13 February 2004)
Corresponding author C. J. Garland: Department of Pharmacy and Pharmacology, University of Bath, Bath BA2 7AY, UK. Email: c.j.garland@bath.ac.uk

Spreading vasodilatation is known to be a significant phenomenon in both the microcirculation and the vasculature of skeletal muscle (Hilton, 1959; Duling & Berne, 1970). In arterioles, dilatation can occur over a considerable distance, reflecting an intrinsic property of the arteriolar wall which enables it to spread along the longitudinal axis of the vessel (Duling & Berne, 1970; Segal & Duling, 1986). However, it is not clear to what extent this phenomenon may operate in larger arteries. In skeletal muscle blood vessels, a proximal spread of dilatation can occur from arterioles through small arteries to the femoral artery (Hilton, 1959). However, in the latter, the dilatation resulting from increases in blood flow (due to downstream dilatation) cannot be fully separated from dilatation spreading from within the microcirculation (Pohl *et al.* 1986; Gustafsson & Holstein-Rathlou, 1999).

In arterioles, it appears that the focal application of dilator agents can only induce a spreading vasodilatation if pathways leading to smooth muscle hyperpolarization are activated (Delashaw & Duling, 1991). This suggests that an increase in membrane potential may be the fundamental signal required to enable spreading dilatation. The endothelium and the single layer of smooth muscle present in arterioles are tightly coupled electrically. Hyperpolarization evoked in the endothelium, with ACh or by the direct injection of current, is mirrored in the smooth muscle cells (Emerson & Segal, 2000*a*; Yamamoto *et al.* 2001), and can spread longitudinally upstream by over 3 mm (Emerson *et al.* 2002). With each stimulus, this hyperpolarization was associated with a dilatation over the entire length of an isolated arteriole (Emerson & Segal, 2000*a*). Interestingly, the spread of both dilatation and

 DOI: 10.1113/jphysiol.2003.060343

the associated hyperpolarizing current depended on the integrity of the endothelium (Emerson & Segal, 2000*b*, 2001; Yamamoto *et al.* 2001). These data indicate a functional role for homo- and heterocellular gap junctions, to enable the spread of hyperpolarization and associated smooth muscle relaxation. The longitudinal orientation of the endothelial cells is ideally suited to provide a low resistance path connecting many circumferentially aligned smooth muscle cells (Haas & Duling, 1997; Emerson & Segal, 2000*a*; Yamamoto *et al.* 2001). However, in larger arteries, the increasing number of smooth muscle layers will present a growing current sink to dissipate the hyperpolarization and thus reduce the extent of longitudinal spread. The functional significance of this current sink will depend on the extent of cellular coupling through gap junctions, but in all likelihood will serve to restrict severely the spread of dilatation.

In small resistance arteries, a considerable body of research has focused on elucidating the mechanisms and importance of local dilatation initiated through the endothelium. In essence, the focus has been on the radial rather than the longitudinal spread of dilatation. The activation of rat mesenteric artery endothelial cells with agonists such as ACh stimulates a rise in endothelial cell $[Ca^{2+}]_i$ (Fukao *et al.* 1997; Dora *et al.* 2000; Oishi *et al.* 2001) and hyperpolarization (White & Hiley, 2000; Tare *et al.* 2002; Hinton & Langton, 2003), which are both associated with hyperpolarization and relaxation in the adjacent smooth muscle cells (Garland & McPherson, 1992). The smooth muscle cell effects are due to the action of a diffusible factor (EDHF) and possibly the spread of hyperpolarization from the endothelium to the smooth muscle through myoendothelial gap junctions (Edwards *et al.* 1998; Doughty *et al.* 2000; Tare *et al.* 2002). In the latter situation, defining the relative importance of current spread from the endothelium to the smooth muscle, which is responsible for relaxation, has proved exceedingly difficult. This is mainly because none of the available gap-junction uncoupling agents are truly selective, and certainly there is no reason to suggest they can preferentially block the myoendothelial junctions. In rat mesenteric resistance arteries, morphological data showing that myoendothelial gap junctions are actually present has significantly strengthened the suggestion that radial electronic coupling may play an important role in local, endothelium-dependent dilatation (Sandow & Hill, 2000). However, there is no direct evidence to indicate if cell–cell coupling can support the longitudinal spread of vasodilatation in a resistance vessel such as the small mesenteric artery. Under isometric or isobaric conditions, rat mesenteric arteries can develop coordinated and rhythmic smooth muscle cell contraction, which reflect changes in muscle membrane potential. This is most clearly observed during stimulation with adrenergic agonists, where oscillations in contraction are associated with, and are immediately preceded by, oscillations in membrane potential (Garland & McPherson, 1992; Gustafsson *et al.* 1993; Wesselman *et al.* 1997; Dora & Garland, 2001; Oishi *et al.* 2002). These closely coordinated changes in artery diameter strongly suggest that the smooth muscle cells are effectively coupled electrically, and might therefore be able to develop and sustain a spreading vasodilatation.

Therefore, the present study was designed to investigate if endothelium-dependent and -independent hyperpolarization associated with arterial relaxation can spread longitudinally over significant distances in rat small isolated resistance arteries. When this was found to be the case, we investigated the potential role of the endothelium in facilitating the spread of dilatation and the possible underlying mechanism.

Methods

Tissue preparation

Male Wistar rats (200–250 g) were killed by cervical dislocation and exsanguination (Schedule 1 procedure; Animals Scientific Procedure Act 1986, UK). The mesenteric arcade was removed and placed in Mops buffer at room temperature. A third-order branch of the superior mesenteric artery was then carefully dissected free of adherent tissue. In all experiments, arteries were superfused continuously with Mops solution containing (mM): 145 NaCl, 4.7 KCl, 2.0 $CaCl_2$, 1.17 $MgSO_4$, 2.0 Mops, 1.2 NaH_2PO_4, 5.0 glucose, 2.0 pyruvate, 0.02 EDTA, 2.75 NaOH, and the pH of the solution was adjusted to 7.39–7.41 at 37°C. All drugs used were purchased from Sigma Chemical Company (Poole, UK). Levcromakalim was a generous gift from Glaxo SmithKline, UK.

Pressure myography

A segment (4 mm long) of mesenteric artery (diameter *ca* 200–300 μm) was cut and then cannulated at each end with a glass pipette (diameter 150 μm) positioned in a small chamber (0.5 ml, custom-made) seated in a heated stage insert (PH-5, Warner instruments). The pipettes were positioned with micromanipulators mounted on stands independent of the microscope. Arteries were continuously superfused with Mops solution (2 ml min^{-1}), which routinely contained the NO synthase inhibitor

L-NAME (10^{-4} M). To avoid luminal flow, the upstream and downstream pressures remained equal throughout the experiment. After equilibration at 37°C for 20 min, arteries were longitudinally stretched with a micrometer during maximal inflation (at 80 mmHg), and then maintained at 50 mmHg for the remainder of experiments. This equated to an optimum axial stretch of 20%, as determined by measuring reactivity to 1 μM phenylephrine, and was consistent with published data (Coats & Hillier, 1999). The pressurized artery was visualized using an inverted microscope (IX70, Olympus UK) and CCD camera (Nikon, Japan), with images stored to videotape. Only arteries without visible side-branches were used, and this usually limited the artery length used for experimentation to 2.0 mm. Artery diameter was displayed online and recorded offline using interactive video calipers (Microcirculation Research Institute, Texas A & M University, USA) linked to a MacLab data acquisition system (ADInstruments Model 4e). A glass micropipette (stimulation pipette; filled with ACh or levcromakalim) was positioned using a micromanipulator independent of the microscope. The pipette was advanced carefully until it just touched the adventitia, then stepped back to a position < 20 μm from the artery. The stimulation pipette remained at the downstream end of the artery, and the upstream sites were visualized by moving the microscope and tissue chamber, using a translation table, along the length of artery (which remained stationary). Arteries were precontracted with 0.1–1 μM phenylephrine, to reduce the resting diameter by *ca* 20%. Dilatation was then expressed as a percentage reversal of this contraction (100% being complete reversal) at the local (0 mm) and distal sites (up to 1.5 mm upstream from the stimulation pipette). When used, Ba^{2+} (30 μM) was added to the Mops superfusion solution and arteries equilibrated for at least 15 min prior to agonist-evoked dilatation.

Selective measurement of endothelial cell $[Ca^{2+}]_i$ change

In separate experiments, following equilibration of pressurized arteries, Mops solution containing the fluorescent indicator fluo-4 AM (50 μg ml^{-1}) was perfused through the artery lumen for 10 min, to enable the selective loading of the dye into endothelial cells. Fluorescence intensity was measured using a laser scanning confocal microscope (FV500-SU, Olympus, Japan, excitation 488 nm, emission 505 nm) and recorded with Tiempo software (Olympus, USA) at 1 Hz. To enable continuous observation of individual endothelial cells, in these experiments the plane of focus was lowered to the endothelial layer, and nifedipine (1 μM) used to dilate arteries maximally (phenylephrine was not added).

Recording of membrane potentials in mesenteric artery smooth muscle cells

A segment (3 mm long) of artery (diameter approximately 200 μm) was fixed with pins to the base of a small tissue chamber (0.5 ml) placed on a bridge stage (Gibraltar, Burleigh, USA) and superfused at 2 ml min^{-1} with Mops solution at 37°C. Both the microelectrode and stimulation pipette were positioned with micromanipulators fixed to the stage. The artery was visualized with an upright microscope (BX50, Olympus UK) placed on a translation table (Gibraltar, Burleigh, USA), allowing 3-D movement independent of the stage. Sharp glass microelectrodes were then used to measure the membrane potential of individual smooth muscle cells. Briefly, a borosilicate glass electrode was back-filled with 2 M KCl solution (tip resistance 50–100 MΩ) and used to impale smooth muscle cells from the adventitial surface of the artery, close to the upstream end. In the majority of experiments, the cell remained impaled for an entire series of local and distal responses, whilst the stimulation pipette was moved from a position adjacent to the intracellular recording electrode (local site) to defined positions downstream (1 mm and 2 mm, distal sites). The pulse duration used to eject either ACh or levcromakalim was varied in order to evoke hyperpolarization of a similar magnitude at the local site with each agent. The membrane potential was recorded via a preamplifier (Neurolog system, Digitimer Ltd, UK) linked to a MacLab data acquisition system (ADInstruments Model 4e) at 100 Hz.

Focal application of drugs

Either ACh (10^{-3} M) or levcromakalim (10^{-3} M) were applied focally from a bevelled borosilicate glass micropipette (5 μm tip) using a pneumatic pico pump (PV 820, World Precision Instruments Inc., FL, USA). The micropipette was always at least 500 μm from the end of the artery. The direction of superfusion of Mops was carefully controlled in all experimental setups. Microspheres (5 μm diameter, Molecular Probes) were routinely added to the superfusion solution to assess the direction of flow and only experiments where the flow was clearly upstream to downstream were used.

Recording of membrane potentials in mesenteric artery endothelial cells

A segment (2–3 mm long) of artery (diameter approximately 200 μm) was cut longitudinally and

fixed with pins to the base of a small tissue chamber (0.5 ml) with the endothelium uppermost. For intracellular recordings, a sharp microelectrode was positioned at approximately 60 deg to the tissue, in order to impale individual endothelial cells. Penetration of an endothelial cell through to the internal elastic lamina was readily detectable, and prevented inadvertent impalement of smooth muscle cells. Injection of dye in some experiments demonstrated that endothelial cells were impaled (see Fig. 9). All drugs were added to the Mops-buffered superfusion solution. The experimental set-up was otherwise identical to intracellular recording of membrane potential from smooth muscle cells.

Recording from isolated endothelial cells

After removal, mesenteric arteries were cleaned of fat and connective tissue, cut longitudinally and placed in Hepes-buffered low-Ca^{2+} physiological saline solution [low-Ca PSS (mM): 136 NaCl, 5.6 KCl, 0.47 $MgCl_2(6H_2O)$, 4.17 $NaHCO_3$, 0.44 $NaH_2PO_4(H_2O)$, 0.42 Na_2HPO_4, 10 Hepes, 0.1 $CaCl_2(2H_2O)$, pH adjusted to 7.4 (NaOH)] containing 1.0 mg ml^{-1} dithiothreitol, 1.0 mg ml^{-1} papain and 1.0 mg ml^{-1} bovine serum albumin. After incubation for 10 min at room temperature followed by 7 min at 37°C, the tissue was transferred to Ca^{2+}-free PSS of the following composition (mM): 124.7 NaCl, 4.8 KCl, 1.73 $MgCl_2$, 1.20 KH_2PO_4, 10 Hepes, 1 EGTA, 11 D-glucose (pH adjusted to 7.4). After washing 3–4 times in Ca^{2+}-free PSS, the cells were dispersed by triturating the tissue with a wide pore pipette. A drop of the cell suspension was then transferred to an experimental chamber, and cells allowed to attach to the glass coverslip for at least 20 min. Single smooth muscle cells were by far the most common cells observed, and were often elongated. The digestion protocol was specifically modified to leave intact sheets of endothelial cells, which could be clearly differentiated from the smooth muscle cells. Throughout experiments, cells were continuously superfused (2 ml min^{-1}) with Hepes-buffered solution containing (mM): 130 NaCl, 5 KCl, 1 $MgCl_2(6H_2O)$, 10 Hepes, 2 $CaCl_2(2H_2O)$, 10 D-glucose (pH adjusted to 7.4), at room temperature.

Membrane potential recordings from the freshly isolated endothelial cells were made using the perforated-patch method of the patch-clamp technique. The pipette solution for perforated-patch recording contained (mM): 130 KCl, 5 MgATP, 0.2 NaGTP, 1 $MgCl_2$, 10 EGTA, 1 $CaCl_2$, 10 Hepes, and 350 μg ml^{-1} amphotericin B (pH adjusted to 7.2).

Assessment of dye coupling

To assess the extent of dye coupling between cells, an artery was mounted with a side branch uppermost. The branch was carefully removed, to leave a small hole through which the endothelial cell layer could be viewed. Endothelial cell impalements were then made with borosilicate glass electrodes filled with the cell membrane-impermeant, low molecular weight dye propidium iodide (1%) dissolved in 2 M KCl solution (Emerson & Segal, 2001). The tip resistances were 100–500 MΩ. Following cell impalement, current injection (1 nA for 1 min) was used to eject, and dye fluorescence (>570 nm) was then recorded using a cooled CCD camera (CoolSnap HQ, Roper Scientific, Munich, Germany). In some experiments, the electrode was passed through the internal elastic lamina to impale the underlying smooth muscle cells. In one experiment, after injection of propidium iodide into an impaled endothelial cell, another cell-impermeant nuclear dye, SYTOX Green (1 nM, Molecular Probes), was added to the superfusion solution to mark all the damaged cells. Fluorescence images were collected at both 405 nm and 570 nm.

Data analysis

Results are summarized as means ± S.E.M. of n replicates. Data were compared using Students's t test. $P < 0.05$ was considered statistically significant. Average diameter values were expressed as a percentage dilatation of phenylephrine-precontracted arteries (complete reversal = 100%). Average changes in $[Ca^{2+}]_i$ (5 individual cells per n) were indicated by the fluorescence intensity (F) divided by the fluorescence intensity recorded immediately before application of agonist ($F_{t=0}$). Average membrane potential data were expressed as both the increase in membrane potential, and the increase in membrane potential from rest over time (area under curves, AUC, mV s). The latter were represented at the AUC at each position along the artery (0–2 mm), divided by the AUC at the local site (AUC_{local}).

Results

Spreading vasodilatation evoked by either ACh or levcromakalim

At 50 mmHg, the mean internal diameter of mesenteric arteries was 299 ± 10 μm (n = 17). All experiments were performed in the presence of the NO synthase inhibitor L-NAME (10^{-4} M), so that the local response to ACh reflected only the activation of the EDHF response (Garland & McPherson, 1992). Only vessels in which

ACh (10^{-6} M in superfusate) was able to reverse contraction to phenylephrine ($1-3 \times 10^{-7}$ M) by $\geq$ 90% were used further. To measure spreading vasodilatation, arteries were contracted by adding a low concentration of phenylephrine to the superfusate solution ($1-3 \times 10^{-7}$ M), which decreased diameter by around 20%. Next, ACh or levcromakalim were applied locally from a pipette positioned at the downstream end of the artery (Fig. 1). Following the application of ACh (10^{-3} M pipette solution, 30 ms at 10 p.s.i.) at the local site, arteries dilated by 65 $\pm$ 14 μm (equivalent relaxation of the phenylephrine constriction, 88 $\pm$ 14%, $n = 6$). This local dilatation to ACh coincided with synchronous dilatation along the entire artery length, with a graded reduction in the extent of dilatation with distance. At 1.5 mm upstream of the stimulation pipette, the arteries dilated by 46 $\pm$ 19%

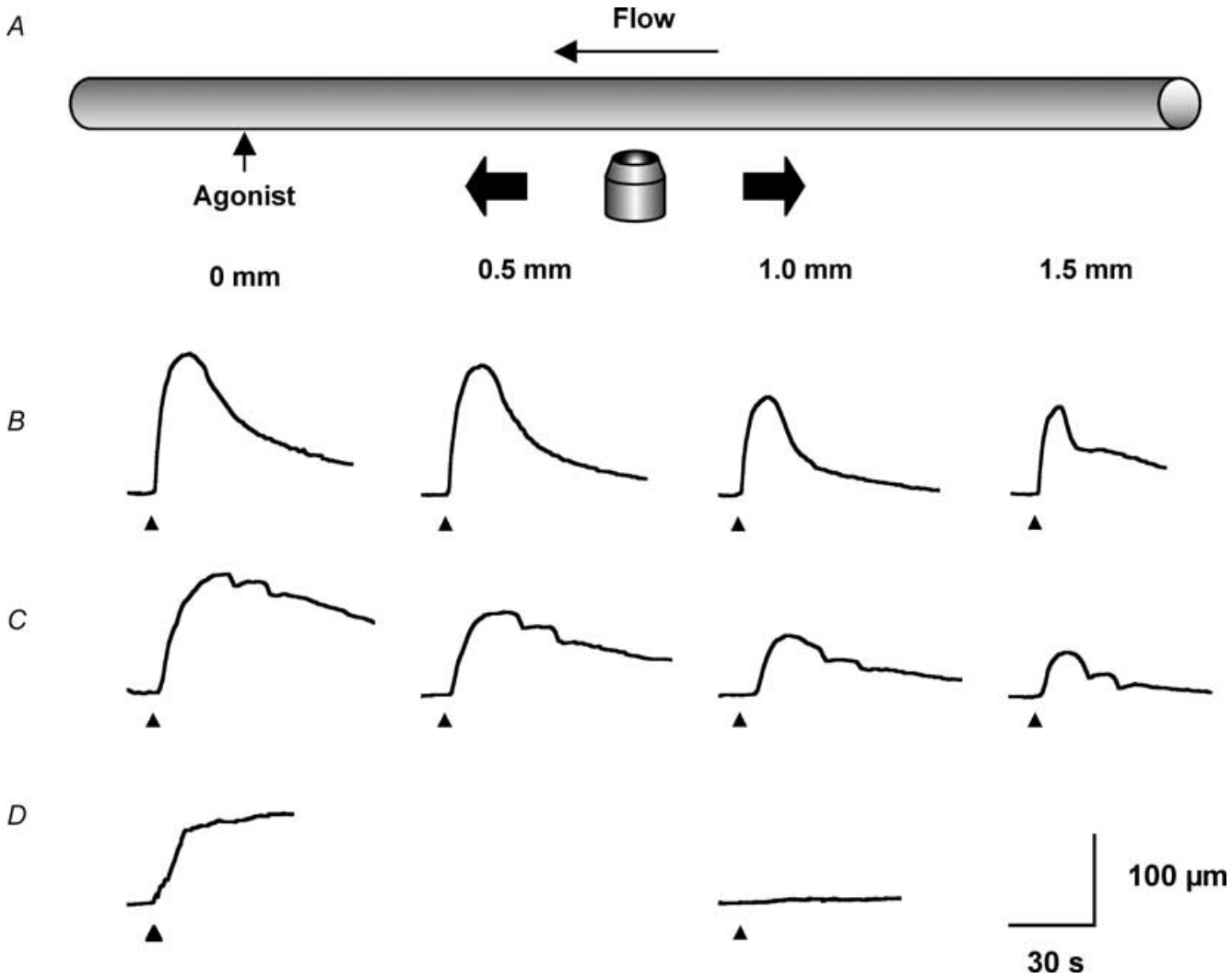

Figure 1. Representative records of local and conducted dilatation in response to agonists
A, schematic diagram of the experimental paradigm in pressurized arteries. Each agonist was pressure-pulse ejected at the local site (0 mm) and the microscope moved independently of the artery and pipette (which remained fixed). This enabled observation of diameter along the artery length whilst maintaining a constant position of stimulation. The superfusion flow prevented the passive diffusion of agonist to the upstream sites. *B–D*, time course of changes in artery diameter in response to local application of agonist at the time indicated by each triangle. The artery dilated rapidly upon focal application of ACh (*B*, 10^{-3} M, 30 ms) and levcromakalim (*C*, 10^{-3} M, 30 ms) at all observation sites along the artery length. For each observation, the artery wall dilated synchronously, with decay in amplitude with distance. *D*, in endothelium-denuded arteries, the duration of levcromakalim stimulation was increased to 300 ms, to evoke local responses of a similar magnitude to responses in endothelium-intact arteries. In these experiments, the dilatation only occurred near the site of stimulation, and by 1 mm upstream no change in diameter was observed.

(Fig. 2, $n = 6$). A very similar profile was observed with levcromakalim, except that the dilatation reversed more slowly than with ACh, usually requiring at least 2 min. Following the local application of levcromakalim (10^{-3} M pipette solution, 30 ms at 10 p.s.i.), arteries dilated by 89 ± 13 μm, which represented a 92 ± 6% reversal of the phenylephrine constriction ($n = 11$). The local dilatation to levcromakalim also coincided with a spreading dilatation that decayed with distance, so that at 1.5 mm upstream from the stimulating pipette, the phenylephrine constriction was reversed by 57 ± 13% (Fig. 2, $n = 9$).

Possible influence of K_{IR} on the spread of dilatation

In a separate series of experiments, the average control dilatation to ACh (30 ms pulse in the presence of L-NAME) at 0 mm was 101.3 ± 25.1% and at 1 mm upstream was 63.0 ± 25.2%. The spreading response to ACh was not altered in the presence of 30 μM Ba^{2+} in the superfusate (0 mm: 122.0 ± 23.2%; 1 mm: 61.6 ± 9.4%, $n = 3$). Similarly, the average control dilatation to levcromakalim (30 ms pulse) was 101.1 ± 1.4% locally and 82.6 ± 29.0% at 1 mm upstream, which was not altered in the presence of Ba^{2+} (0 mm: 110.5 ± 8.0%; 1 mm: 90.0 ± 7.5%, $n = 3$).

Influence of the endothelium on the spread of dilatation

To investigate the possible role of the endothelium in facilitating spreading dilatation, these cells were disrupted by gently rubbing the luminal surface of artery segments with a human hair, before they were mounted for pressure myography. In this experimental series, the resting diameter of the arteries was 295 ± 28 μm ($n = 3$), which was not different from the endothelium intact vessels. In the endothelium-denuded arteries, the contraction in response to phenylephrine was not uniform, with fusiform regions of contraction along the artery length. Furthermore, synchronized oscillations in diameter in response to phenylephrine were never observed in these vessels. This was in marked contrast to the endothelium-intact arteries, where the entire artery length always contracted uniformly to phenylephrine, and rhythmic oscillations were often observed. Endothelium-denuded arteries did not relax in response to acetylcholine (1–3 × 10^{-6} M added to the tissue chamber). In contrast, levcromakalim acted directly on the smooth muscle cells so dilatation was maintained in the absence of endothelium. In endothelium-denuded arteries, the local dilatation in response to levcromakalim (10^{-3} M pipette solution, 30 ms at 10 p.s.i.) was found to be reduced compared to

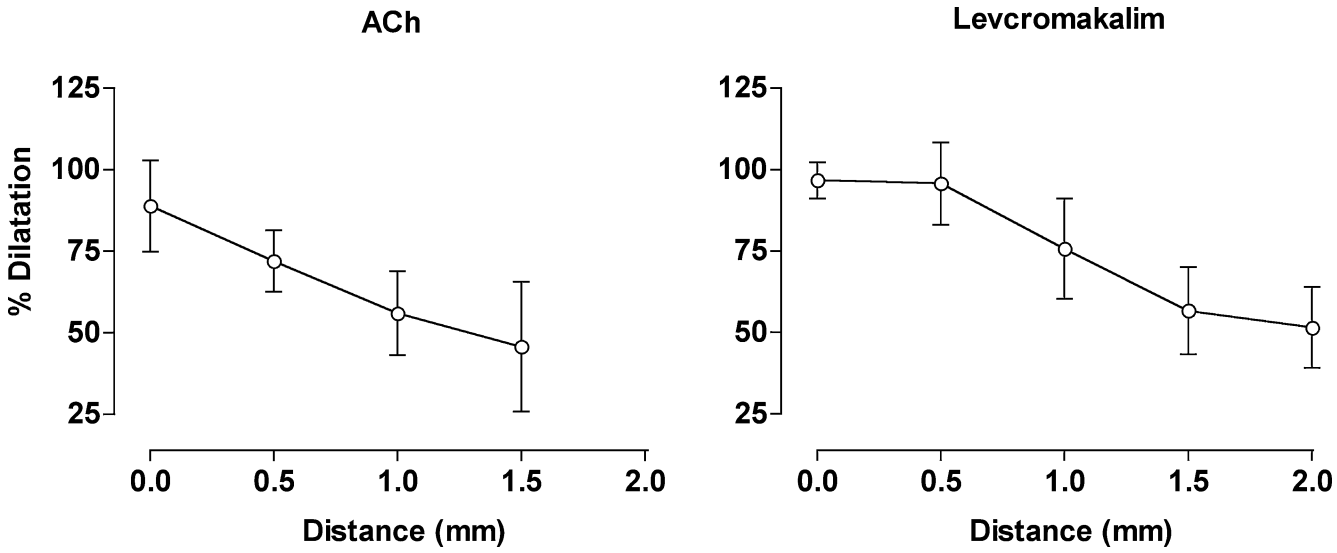

Figure 2. Local and conducted dilatation evoked by ACh and levcromakalim
Summarized data showing the average peak increase in diameter (% dilatation) along the artery length stimulated by ACh (left panel, $n = 6$) and levcromakalim (right panel, $n = 6$–11). Both agonists were pressure-pulse ejected (10^{-3} M for 30 ms) at the local site (0 mm) and changes in diameter were observed at sites upstream and against the direction of superfusion flow. All arteries were precontracted with phenylephrine (1–3 × 10^{-7} M) to stimulate approximately 20% tone.

the endothelium-intact arteries (44 ± 10%, $n = 4$, *versus* 92 ± 6%, $n = 11$), so the duration of levcromakalim ejection was increased 10-fold (to 300 ms) to evoke dilatation of greater magnitude at the local site (68.4 ± 9.0%, $n = 3$). In this separate series, no significant spread of dilatation occurred. The local dilatation tapered steeply toward the upstream portion of the artery, at 1 mm upstream only a small dilatation equivalent to only 6.6 ± 6.6% reversal of the phenylephrine constriction was observed ($n = 3$, Fig. 3). To rule out the possibility that the attenuation of spreading dilatation was due to the reduced size of the initial local dilatation, endothelium-intact arteries from the same animal were used as controls. In these experiments, the duration of stimulation was reduced (10–30 ms) to obtain a comparable local dilatation (69.2 ± 3.9%, $n = 3$) to denuded arteries. In these vessels, dilatation spread along the artery with only a modest, gradual decay, so at 1 mm upstream, the artery dilated by 50.7 ± 8.5% ($n = 3$, Fig. 3).

Extent of spread of changes in endothelial cell $[Ca^{2+}]_i$

In pressurized mesenteric arteries, the Ca^{2+} indicator fluo-4 was selectively loaded into the endothelial cells by luminal perfusion (Fig. 4*A*). Again, the NO synthase inhibitor L-NAME (10^{-4} M) was present throughout. To assess the

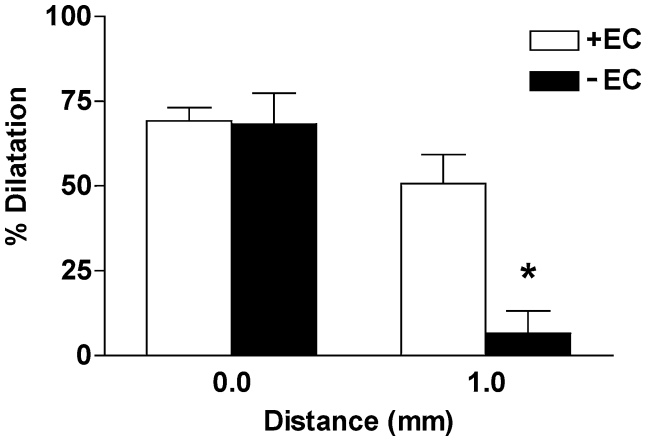

Figure 3. The endothelium facilitated conducted dilatation in response to levcromakalim
Summarized data showing the average peak increase in diameter (% dilatation) stimulated by levcromaklim in endothelium-intact (+EC, $n = 3$) and endothelium-denuded (–EC, $n = 3$) arteries. The duration of focal (at 0 mm) pressure-pulse ejection was titrated to obtain similar magnitudes of local dilatation. At 1 mm upstream from the stimulation pipette the amplitude of dilatation was markedly reduced in the denuded artery, supporting the crucial importance of the endothelium in facilitating the spread of dilatation. All arteries were precontracted with phenylephrine ($1–3 \times 10^{-7}$ M) to stimulate approximately 20% tone. $^*P < 0.05$ *versus* +EC at 1 mm.

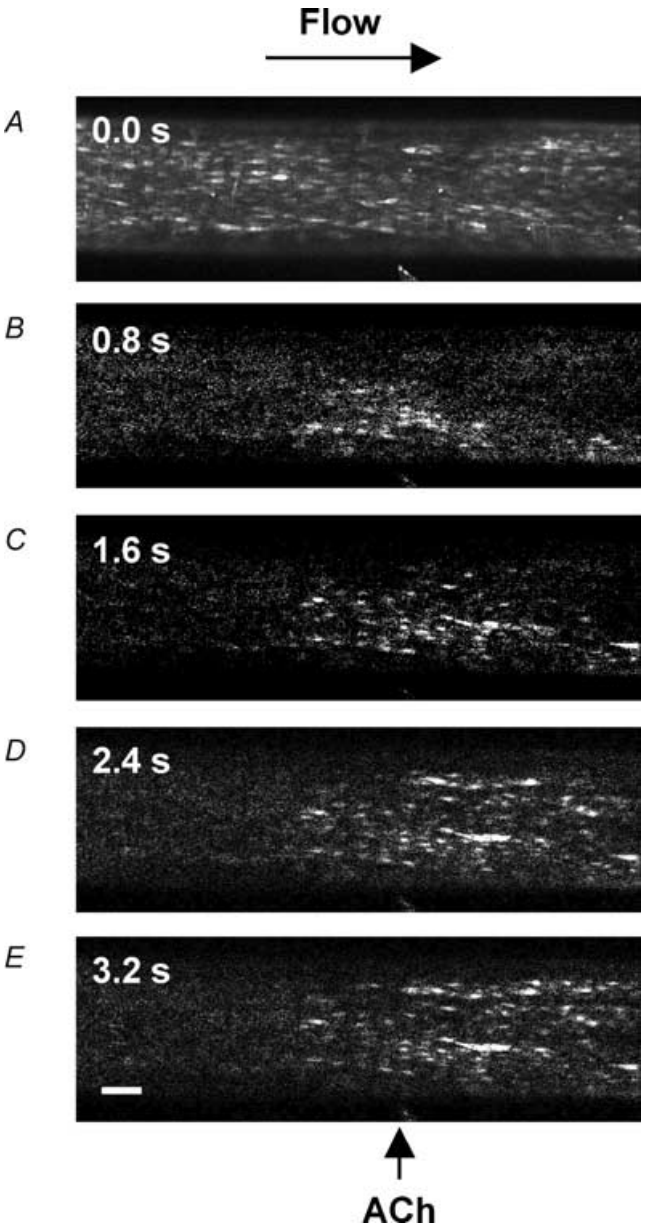

Figure 4. Representative images of local and conducted changes in endothelial cell $[Ca^{2+}]_i$ in response to ACh
Pressurized arteries were luminally loaded with the fluorescent Ca^{2+} indicator fluo-4 selectively to load endothelial cells. *A*, fluorescence image of the lower wall of the artery at the plane of the endothelial cells, equivalent to $F_{t=0}$. The position of the stimulation pipette is visible at the bottom of the image (also indicated by arrow in *E*) and the flow of superfusate are is from left to right to avoid upstream diffusion of ACh. *B–E*, sequential $F/F_{t=0}$ images of the same artery, where ACh was pressure-pulse ejected (10^{-3} M, 300 ms) at $t = 0$ s, and *F* acquired at the times indicated in the top left of each image. Note that in *B* the rise in endothelial cell $[Ca^{2+}]_i$ occurred in the vicinity of the pipette, and subsequently (*C–E*) spread both downstream (longitudinally) and across (radially) the artery wall, but not to regions beyond 400 μm upstream of the pipette. Addition of ACh (10^{-6} M) to the bath increased endothelial cell fluorescence intensity across the entire length of artery (not shown). Bar = 100 μm.

viability of endothelial cells along the length of the artery segment, ACh (10^{-6} M) was added to the tissue bath. ACh increased fluorescence intensity ($F_{peak}/F_{t=0}$) by 2.06 ± 0.51, 1.81 ± 0.38 and 1.87 ± 0.35 ($n = 6$) within endothelial cells at points 0, 0.25 mm and 0.5 mm distant from the stimulation pipette, respectively. These positions were subsequently used to assess the extent of spread of Ca^{2+} increases in the endothelium.

Focal application of ACh (10^{-3} M pipette solution, 300 ms at 10 p.s.i.) stimulated a transient and localized increase in the intensity of fluorescence of the endothelial cells ($F_{peak}/F_{t=0} = 1.22 \pm 0.33$, $n = 14$). This increase in fluorescence returned to the resting prestimulation level within 10 s (Figs 4 and 5). Increases in fluorescence intensity of the endothelial cells could also be detected at 0.25 mm upstream from the stimulating site ($F_{peak}/F_{t=0} = 1.06 \pm 0.02$, $n = 14$). However, no significant change was detected by 0.5 mm upstream of the point of application of ACh ($F/F_{t=0} = 1.01 \pm 0.01$, $n = 14$).

The local application of levcromakalim (10^{-3} M pipette solution, 100 ms at 10 p.s.i.) did not have any effect on the endothelial cell calcium concentration, at either the local or upstream sites (Fig. 5).

Spread of smooth muscle hyperpolarization evoked with ACh and levcromakalim

In the presence of L-NAME, smooth muscle cells had a resting membrane potential of −51.7 ± 1.4 mV ($n = 20$). The application of either ACh (3×10^{-6} M) or levcromakalim (10^{-6} M) to the tissue bath, evoked a hyperpolarization of 20.1 ± 1.8 mV ($n = 6$), and 24.0 ± 1.9 mV ($n = 3$), respectively.

The subsequent focal application of ACh (10^{-3} M, 5–100 ms at 10 p.s.i.) stimulated a transient smooth muscle hyperpolarization at the site of pressure ejection, with a peak amplitude of 12.7 ± 1.2 mV (AUC = 233 ± 46 mV s, $n = 10$). A significant smooth muscle hyperpolarization in response to the focal application of ACh could be recorded at all positions up to 2 mm upstream from the stimulating pipette (peak amplitude at 0.5 mm: 7.2 ± 2.2 mV; at 1.0 mm: 6.1 ± 1.2 mV, $n = 5$–7, and at 2 mm: peak amplitude of 3.6 ± 0.4 mV; $AUC/AUC_{local} = 0.19 \pm 0.04$; $n = 4$ Figs 6 and 7). The spread of hyperpolarization evoked in response to ACh was blocked by carefully cutting the artery at a point approximately 200 μm upstream from the stimulating pipette. The artery was cut completely in half between very small tungsten pins which held the cut ends

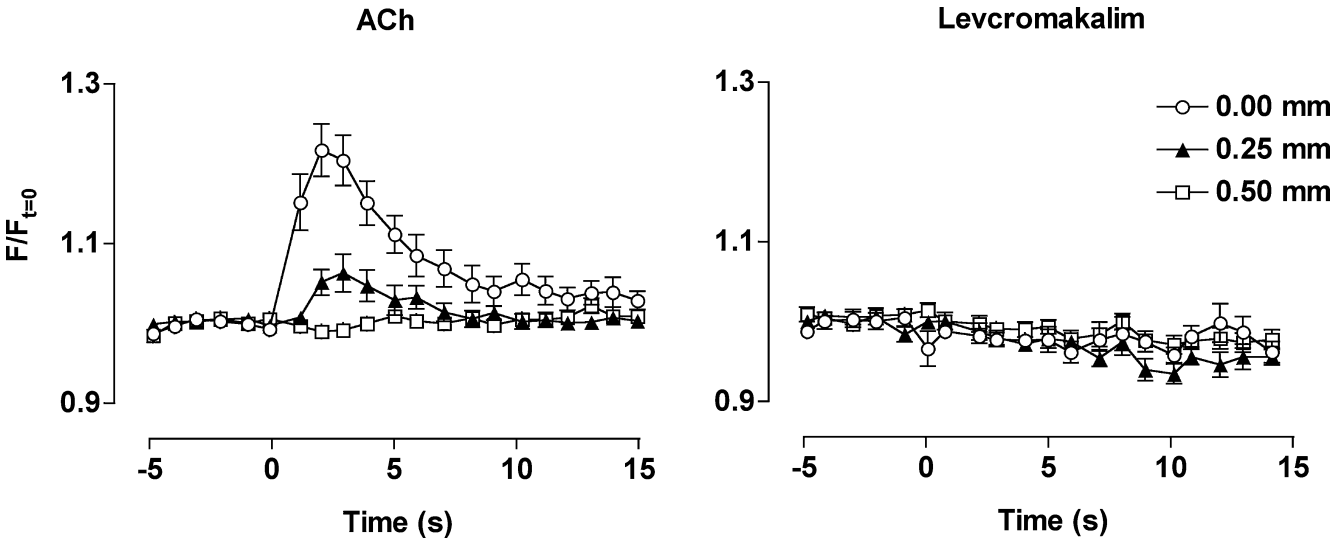

Figure 5. Local and conducted changes in endothelial cell $[Ca^{2+}]_i$ in response to ACh and levcromakalim
Summarized data showing the average time course of changes in fluorescence intensity ($F/F_{t=0}$) stimulated by ACh (left panel, $n = 14$) and levcromakalim (right panel, $n = 15$) along the artery length. Both agonists were pressure-pulse ejected (10^{-3} M, 300 or 100 ms, respectively) at the local site (0 mm) and changes in fluorescence observed at sites upstream and against the direction of superfusion flow. Note that a rise in endothelial cell $[Ca^{2+}]_i$ only occurred in response to ACh, and only in regions less than 500 μm upstream of the stimulation pipette. Phenylephrine was not present in these experiments.

in position approximately 20 μm apart. After cutting the artery, while the local peak hyperpolarization to ACh was unaffected (12.7 ± 2.4 mV, $n = 3$), no hyperpolarization was recorded above the cut, at 0.5 mm distant from the stimulation pipette (Fig. 7).

Focal pressure ejection of levcromakalim (10^{-3} M, 10–30 ms at 10 p.s.i.) also transiently hyperpolarized mesenteric artery smooth muscle cells (peak = 13.5 ± 4.7 mV). However, the responses were more prolonged than with ACh, with the membrane potential returning to resting level within 3 min (AUC = 2413 ± 601 mV s, $n =$ 10, Figs 6 and 7). The hyperpolarization to levcromakalim spread along the artery, so at 2 mm upstream from the point of application it had a similar magnitude to the hyperpolarization with ACh (peak amplitude 2.6 ± 0.9 mV; $AUC/AUC_{local} = 0.24 \pm 0.9$, $n = 4$; peak amplitude at 0.5 mm: 7.6 ± 1.0 mV; at 1 mm: 4.8 ± 0.6 mV, $n = 6$–7).

In the endothelium-denuded mesenteric arteries, the resting membrane potential was −55.9 ± 0.8 mV ($n =$ 3), and ACh did not evoke any hyperpolarization. Hyperpolarization in response to levcromakalim was not altered

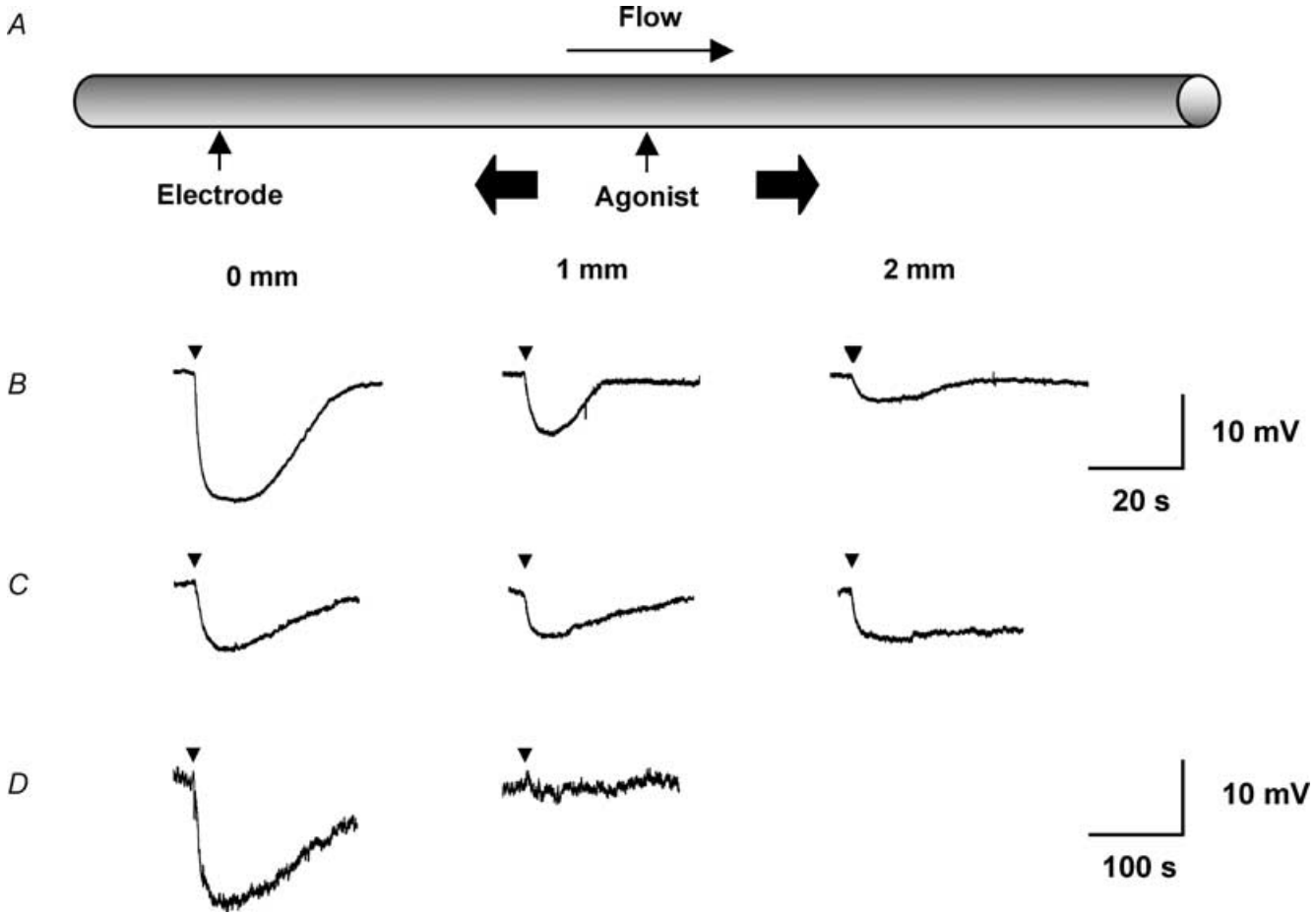

Figure 6. Representative records of local and conducted hyperpolarization to agonists
A, schematic diagram of the experimental paradigm in pinned-out arteries. A smooth muscle cell was impaled with a glass microelectrode at the local site (0 mm) and the position of the stimulation pipette moved independently of the artery and microelectrode (which remained fixed). This enabled measurement of membrane potential at increasing distance from the stimulation pipette during a single impalement. The superfusion flow prevented the passive diffusion of agonist to the upstream sites. *B*–*D*, time course of changes in membrane potential in response to local application of agonist at the time indicated by each triangle. The artery hyperpolarized rapidly upon focal application of ACh (*B*, 10^{-3} M, 5 ms) and levcromakalim (*C*, 10^{-3} M, 20 ms) at all observation sites along the artery length, with decay in amplitude with distance. *D*, in endothelium-denuded arteries, the duration of levcromakalim stimulation was increased to 30 ms, to evoke local responses of a similar magnitude to those in endothelium-intact arteries. In these experiments, the magnitude of hyperpolarization relative to the local response (AUC/AUC_{local}) decreased markedly with distance compared to the endothelium-intact arteries. Note that the time scale for *A* is different to *B* and *C*.

at the local site, but now there was no hyperpolarization at points away from the stimulating pipette. At the local site, the hyperpolarization in response to levcromakalim was similar to the endothelium-intact arteries (peak = 20.0 ± 1.3 mV, AUC = 2133 ± 237 mV s, $n = 3$), indicating that the integrity of the smooth muscle cell layer had not been affected. However, no change in membrane potential was recorded at 1 mm upstream of the point of application (Figs 6 and 7) (peak amplitude 0.4 ± 0.4 mV; $AUC/AUC_{local} = 0.02 \pm 0.02$, $n = 3$). As well as revealing the crucial importance of the endothelium in the ability of the arteries to conduct the hyperpolarization longitudinally, the lack of any significant spread provides further evidence that the agonist was not diffusing to stimulate the upstream sites directly. Equivalent experiments were not possible with ACh, which acts solely through the endothelium.

Levcromakalim stimulates smooth muscle, not endothelial cell K_{ATP}

Intracellular microelectrode recording from endothelial cells *in situ* in isolated mesenteric arteries gave a resting membrane potential of −51.0 ± 1.3 mV ($n = 5$), which was very similar to the smooth muscle cell membrane potential. Levcromakalim increased this potential to −72.4 ± 3.1 mV ($n = 5$), an effect blocked in the presence of the K_{ATP} inhibitor glibenclamide (10^{-5} M, $n = 4$, Figs 8*A* and *B*). However, this hyperpolarization was evoked indirectly, as levcromakalim did not have any effect when applied directly to freshly isolated mesenteric artery endothelial cells. In isolated endothelial cells, ACh (3×10^{-6} M) evoked a reproducible hyperpolarization of around 33 mV in perforated patch-clamp recordings (Fig. 8*C*). In the same cells, levcromakalim had no effect on membrane potential.

Dye spread between cells in the mesenteric artery

Individual smooth muscle or endothelial cells were impaled with a glass microelectrode containing 1% propidium iodide, and current (1 nA for 1 min) used to inject the dye. Impalements on the luminal surface of mesenteric arteries resulted in extensive dye spread between longitudinally orientated cells, whose appearance was consistent with endothelial cells (Fig. 9*A*, $n = 6$).

Cell impalement through the adventitial surface revealed cells with fluorescent elongated nuclei, circumferentially aligned within the artery (Figs 9*B*, $n = 3$). The position, appearance and alignment were all consistent with that expected of smooth muscle cells. The spread of the dye between these cells was

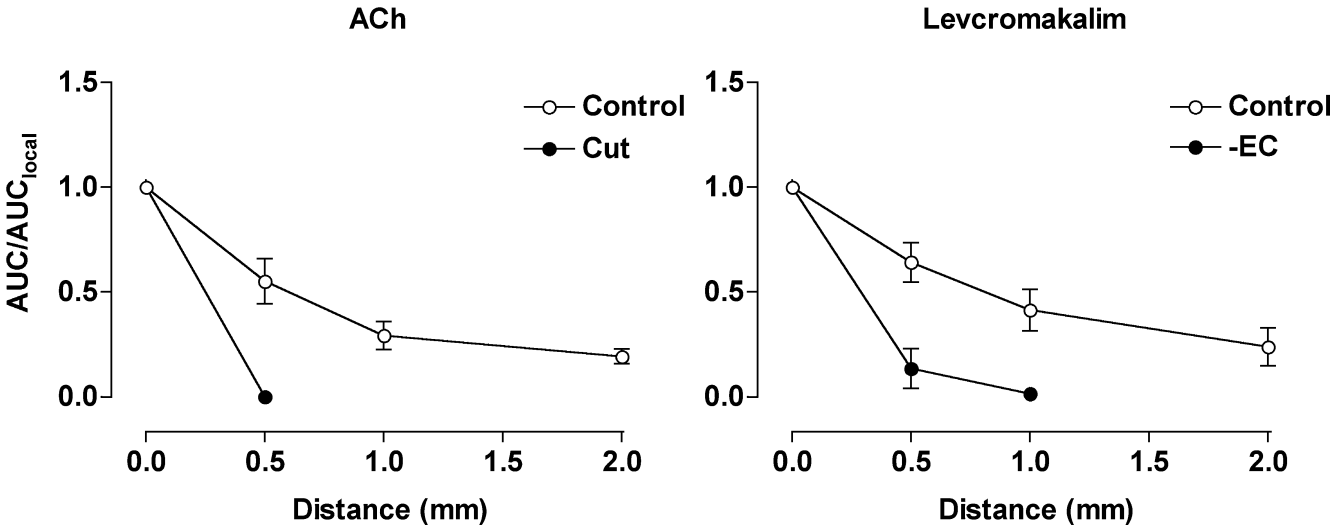

Figure 7. Local and conducted hyperpolarization evoked by ACh and levcromakalim
Summarized data showing the average increase in membrane potential with time (AUC, mV s) along the artery length relative to the local AUC (AUC/AUC_{local}). Both agonists were pressure-pulse ejected at positions along the artery (0–2 mm from microelectrode) and membrane potential recorded at the local site (0 mm). The spread of hyperpolarization in response to ACh (10^{-3} M, 5–100 ms) observed under control conditions (left panel, $n = 4$–9) was abolished by cutting the artery 200 μm downstream from the recording electrode (cut, $n = 2$). The spread of hyperpolarization in response to levcromakalim (10^{-3} M, 10–30 ms) under control conditions (right panel, $n = 4$–10) was markedly reduced in endothelium-denuded arteries (– EC, $n = 3$). Phenylephrine was not present in these experiments.

very restricted compared to the endothelial cells. In one case (of 3 experiments), following impalement and loading of fluorescent dye into a smooth muscle cell, an endothelial cell was also stained. This suggested functional heterocellular coupling within the artery wall.

In two (of six) impalements on the luminal surface of mesenteric arteries fluorescent dye also spread to cells running at approximately right-angles to the endothelial cells (Fig. 9*C*). This suggested spread from the endothelium to the underlying smooth muscle cells. The addition of SYTOX Green (1 nM) to the superfusion solution clearly and discretely stained a small number of individual cells, presumably indicating damaged cells (and all the cells at the cut edge of the tissue; not shown). However, only occasionally were the cells stained by propidium iodide costained also with SYTOX Green (Fig. 9*D*).

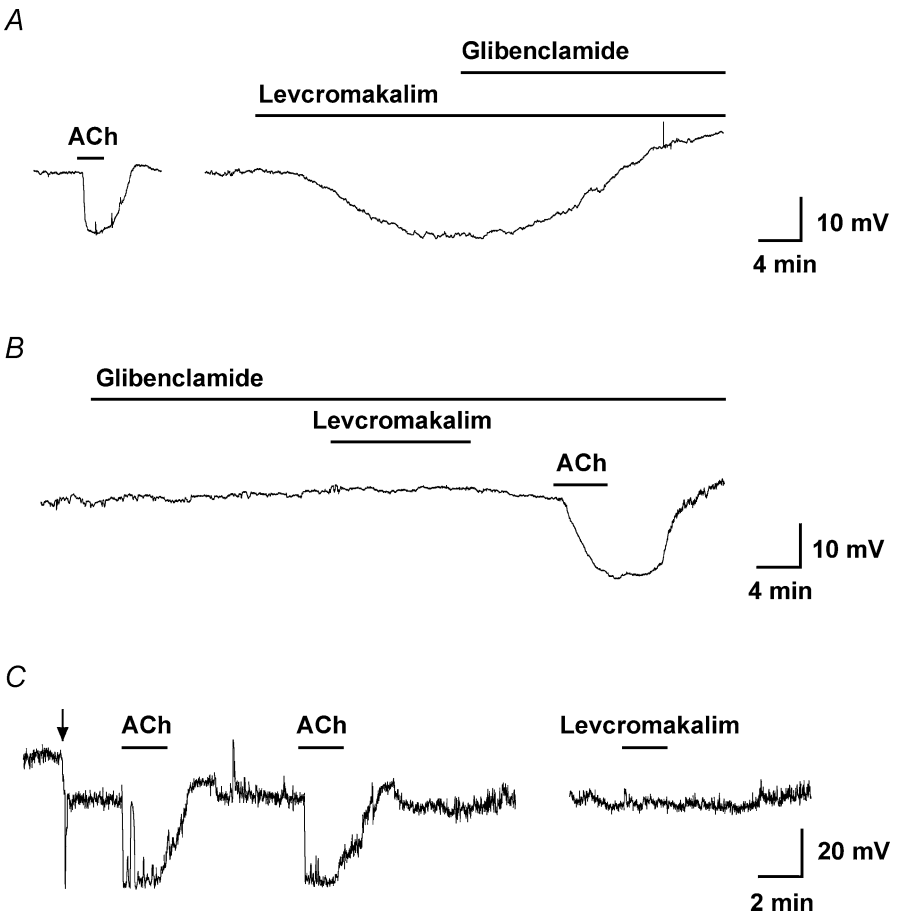

Figure 8. Representative records of endothelial cell hyperpolarization to agonists
Time course of membrane potential change in response to either ACh or levcromakalim in the superfusate. *A* and *B*, intracellular microelectrode records of endothelial cell membrane potential from intact arteries. In *A*, both ACh (10^{-5} M) and levcromakalim (10^{-6} M) stimulated hyperpolarization. The subsequent addition of glibenclamide (10^{-5} M) fully reversed the levcromakalim response. The resting membrane potential in this cell was −54.0 mV. In a separate experiment (*B*), prior application of glibenclamide blocked the hyperpolarization to levcromakalim, but not to ACh. The resting membrane potential was −53.7 mV. On average, membrane potential increased from -50.4 ± 1.1 mV to -68.8 ± 2.2 mV with ACh, and from -51.0 ± 1.3 to -72.4 ± 3.1 mV with levcromakalim ($n = 5$). *C*, measurement of membrane potential in a freshly isolated endothelial cell with a patch-electrode. In contrast to intact arteries, levcromakalim did not evoke hyperpolarization. The resting membrane potential of the isolated endothelial cells was −13.6 mV, which was increased to −32.4 mV by current injection (at the point indicated by the arrow). ACh (3×10^{-6} M) hyperpolarized these cells to −66.1 and −66.6 mV (first and second additions), whereas in the same cell levcromakalim (10^{-5} M) had no effect. The period of agonist and antagonist addition is indicated by bars.

Discussion

The phenomenon of spreading dilatation is clearly recognized within the microcirculation. Here we demonstrate that a similar spreading dilatation can also occur over relatively large distances in a small resistance artery, the rat mesenteric artery. The spreading vasodilatation evoked with either ACh or levcromakalim appears to follow the spread of a hyperpolarizing current, which is dependent on the integrity of the endothelium. This spread does not reflect any regenerative change in endothelial cell $[Ca^{2+}]_i$. Together, these data demonstrate effective electrical coupling between cells of the artery wall which depends on the endothelium. As such, the endothelium provides an underlying means to coordinate vascular responses in resistance arteries, as it does within the microcirculation.

Despite the many early reports of spreading dilatation (e.g. Hilton, 1959), our understanding of this phenomenon did not advance until the use of intravital microscopy enabled direct observations to be made in the microcirculation during agonist application at a defined point from a micropipette (Duling & Berne, 1970). Since that time, investigation of spreading dilatation has almost exclusively utilized endothelium-dependent agonists, predominantly ACh, which evokes a robust dilatation spreading bi-directionally along the length of arterioles (Duling & Berne, 1970; Segal & Duling, 1986; Segal & Beny, 1992; Kurjiaka & Segal, 1995) and small arteries in skeletal muscle (Emerson & Segal, 2000*b*). In contrast, many other vasodilators do not have this effect (Delashaw & Duling, 1991; Gustafsson & Holstein-Rathlou, 1999). However, it is not clear if this is a general characteristic of the blood vessel wall.

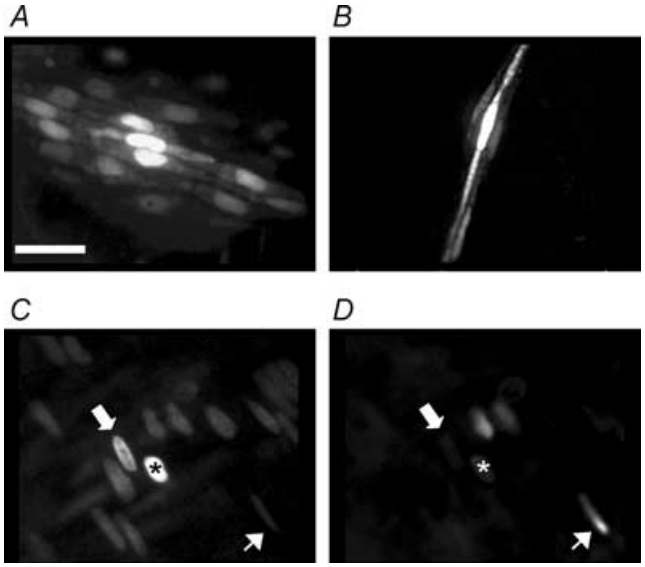

Figure 9. Assessment of homocellular and heterocellular coupling by dye injection

A single endothelial cell (*A*,*C*) or smooth muscle cell (*B*) was impaled with a glass microelectrode containing propidium iodide (1%). Dye appeared to pass more readily to adjacent endothelial cells than to adjacent smooth muscle cells, and on two occasions (from 6) passed from an endothelial cell to underlying smooth muscle cell. *C* and *D*, images collected showing propidium iodide staining (*C*), and then SYTOX Green staining of the same region (*D*). The injected cell is marked by the asterisk, where the resting membrane potential was −52 mV. The thick (upper) arrows point to a cell where propidium iodide fluorescence is evident in a cell adjacent to the injected cell (*C*), but no SYTOX Green fluorescence was observed in the same cell (*D*, suggesting dye-coupling), whereas the thin (lower) arrows show SYTOX Green staining a damaged cell (*D*) which has very low intensity in *C*. Bar = 50 μm.

A number of observations suggest that the spread of hyperpolarizing current is the most likely explanation for spreading vasodilatation. First, the cells with the walls of isolated arterioles were shown to be very tightly coupled electrically (Hirst & Neild, 1978). Second, ACh stimulates endothelial cell hyperpolarization in arterioles and small feed arteries which spreads rapidly to the smooth muscle cells (Yamamoto *et al.* 1999; Emerson & Segal, 2000*a*; Yamamoto *et al.* 2001). Third, this hyperpolarization can spread upstream from the point of stimulation (Emerson & Segal, 2000*a*,*b*; Dora *et al.* 2003). Finally, agonists which stimulate dilatation without causing smooth muscle cell hyperpolarization, such as sodium nitroprusside (Dora *et al.* 2003), do not evoke a spreading dilatation (Delashaw & Duling, 1991; Kurjiaka & Segal, 1995; Doyle & Duling, 1997; Rivers *et al.* 2001) or increases in blood flow (Kurjiaka & Segal, 1995).

As the available evidence from arterioles supports the concept that smooth muscle cell hyperpolarization is an important, probably critical, aspect of spreading dilatation, we have used two different agonists to evoke smooth muscle cell hyperpolarization in the mesenteric artery – ACh acts indirectly to hyperpolarize the smooth muscle by acting on the endothelium, while levcromakalim directly stimulates smooth muscle hyperpolarization. ACh hyperpolarizes the smooth muscle by first activating endothelial cell muscarinic receptors leading to an increase in Ca^{2+} (Busse *et al.* 1988), an effect known to occur in rat mesenteric arteries (Fukao *et al.* 1997; Dora *et al.* 2000; Oishi *et al.* 2001), leading to the activation of endothelial cell K_{Ca} (Walker *et al.* 2001) and subsequent hyperpolarization of the endothelium (White & Hiley, 2000; Tare *et al.* 2002; Hinton & Langton, 2003). The hyperpolarization reflects the activation of small- and intermediate-conductance K_{Ca} channels (Edwards *et al.* 1998; White & Hiley, 2000; Hinton & Langton,

2003). The resulting smooth muscle hyperpolarization and relaxation is inhibited by the combination of apamin and charybdotoxin (Chen & Cheung, 1997) or apamin and TRAM-34 (Crane *et al.* 2003*a*) which inhibit small- and intermediate-conductance K_{Ca}, respectively.

In contrast to ACh, levcromakalim acts directly to hyperpolarize the rat mesenteric artery smooth muscle by opening ATP-sensitive K channels (K_{ATP}), and only appears to hyperpolarize the endothelial cells indirectly, possibly via myoendothelial electrical coupling (White & Hiley, 2000). Our present data now confirm and extend these studies, showing that levcromakalim hyperpolarizes the endothelium in intact rat mesenteric artery, but is unable to directly hyperpolarize these cells.

Longitudinal spread of vasodilatation and hyperpolarization evoked by either ACh or levcromakalim

We show for the first time that spreading dilatation and hyperpolarization can occur in rat small mesenteric arteries. Furthermore, spread of hyperpolarization, and of the associated dilatation, was independent of the cell type in which the response was initiated at the local site. Similar spread of both hyperpolarization and dilatation occurred whether initiated in the endothelium, by the activation of K_{Ca} channels with ACh, or in the smooth muscle by the activation of K_{ATP} channels with levcromakalim. In each case, the response spread to sites over 1.5 mm upstream from the point of stimulation, and with a very similar rate of decay. Overall, the coordinated dilatation along the length of these arteries suggests a rapid pathway of cell-to-cell communication, most likely involving the spread of a hyperpolarizing current.

If hyperpolarization is responsible, it is interesting that spreading responses can occur over such a large distance, as cable theory would predict a rapid decay of hyperpolarization. For example, in arterioles the space constant for decay of injected current is only just over a millimetre (Hirst & Neild, 1978). However, the ability of ACh to stimulate hyperpolarization which spreads to a similar extent as in the present study has also been observed in arterioles (Emerson *et al.* 2002). In these studies, two cells separated by a known distance were simultaneously impaled with microelectrodes. The resulting changes in membrane potential showed that the length constants (λ) were greater during stimulation with ACh (λ_{ACh}), when compared to current injection alone (λ_I). This was in spite of the fact that a local initiating hyperpolarization of equivalent amplitude was evoked in each case. Further, λ_{ACh} was not reduced in longer lengths of arteries (Emerson *et al.* 2002), but λ_I did decrease (Hirst & Neild, 1978; Emerson *et al.* 2002). Thus, it seems that the spread of agonist-induced hyperpolarization is somehow actively facilitated. This may not necessarily reflect an active regenerative mechanism *per se*, but could be due to additional signalling pathways which can influence the coupling between the endothelial cells, as suggested from experiments on cells in culture (Popp *et al.* 2002).

Similar mechanisms could explain our data in rat mesenteric arteries. One possibility is that the opening of K_{IR} along the endothelial cell layer might contribute, as suggested in coronary arterioles (Rivers *et al.* 2001). In the rat mesenteric artery, functional K_{IR} channel activity is restricted to the endothelial cells (Dora & Garland, 2001; Crane *et al.* 2003*b*), which would be consistent with this possibility. However, the activation of these channels alone cannot account for the distal responses in our study, as inhibition of K_{IR} with Ba^{2+} had no effect on the spreading dilatation in response to either ACh or levcromakalim. A possible contribution from other K^+ channels in these arteries will require further investigation.

It seems unlikely that spreading dilatation simply follows dilatation at the local site due to increases in flow through the artery lumen causing flow-dependent dilatation upstream. Although flow-induced dilatation has been observed in this artery (Thorsgaard *et al.* 2003), it cannot be the primary explanation for the spread of dilatation because hyperpolarization spread through the artery wall in the pinned-out preparation, which had no luminal flow and did not change diameter. Furthermore, in the pressurized arteries, the spread of dilatation actually decayed upstream from the pipette, yet at these upstream sites the fluid shear stress would be greater (due to a higher fluid velocity and the smaller diameter). Finally, our studies on spreading dilatation were all performed in the presence of L-NAME, ruling out any significant contribution from NO released by the endothelium, which is thought to be the main mediator of flow-induced dilatation in this and other arteries (Thorsgaard *et al.* 2003).

Role of the endothelium in the spread of dilatation and hyperpolarization

The importance of the endothelium in facilitating the spread of both dilatation and hyperpolarization in the mesenteric artery was very clear. While removal of the endothelium did not prevent the artery from responding to smooth muscle cell-specific vasoconstrictors and dilators *per se*, the dilatation was now only observed in the region of focal application of levcromakalim. This resulted in a

fusiform appearance, reflecting local dilatation without an additional spreading component. Even when the duration of levcromakalim application was increased 10-fold, spread was still not observed.

While it is clear the endothelium is crucial in the spread of dilatation, these data also rule out the possibility that levcromakalim diffuses upstream, or that perivascular nerves might contribute. The profile of dilatation in response to levcromakalim was mirrored by the intracellular membrane potential measurements in pinned-out arteries, as removal of the endothelium blocked the spread of hyperpolarization from the local site. Furthermore, they show that the smooth muscle cell layers cannot contribute significantly to the spread of hyperpolarization away from the local site in a longitudinal direction.

Overall, these data are consistent with studies in arterioles, where the coupling between smooth muscle cells is either poor or known to be prevented by selective light-dye damage to cells in the vessel wall. Here, the pathway for the spread of a hyperpolarizing signal depends on a functional endothelium (Emerson & Segal, 2000*b*, 2001; Yamamoto *et al.* 2001). With coupled cells, the orientation will have a significant impact on the ability of current to spread longitudinally through the artery wall. Endothelial cells are aligned longitudinally and at approximately right angles to the circumferentially orientated vascular smooth muscle cells. As a consequence, one endothelial cell spans around 20 smooth muscle cells (Haas & Duling, 1997). In small arteries, the input resistance of endothelial and smooth muscle cells are almost identical, reflecting heterocellular coupling (Emerson *et al.* 2002). So, simply on the basis of electronic spread, a given hyperpolarization will spread further along the artery by passing through the endothelium than by passing through the circumferentially orientated muscle.

What is the basis of cell–cell coupling?

While the endothelial cells in rat mesenteric arteries have been suggested to contain connexins 37, 40, and 43 (Gustafsson *et al.* 2003), the connexin composition of functional homo- and heterocellular (myoendothelial) gap junctions is not known. The precise connexin composition may well be a crucial determining influence on the spread of vasodilatation. In studies with cremasteric arterioles from connexin 40-deficient mice (this connexin is normally confined to the endothelial cells) the spreading vasodilatation evoked by either ACh (de Wit *et al.* 2000) or electrical stimulation (Figueroa *et al.* 2003) was greatly reduced or abolished. Investigating whether the endothelial cells still hyperpolarize at the upstream sites in these arterioles would indicate if connexin 40 is crucial for functional homo- and/or heterocellular coupling.

However, the ability of depolarization or hyperpolarization to pass longitudinally through the arterial media seems to be extremely limited. For example, in the carotid artery *in situ*, local damage by needle prick induces a powerful ring of localized contraction (Graham & Keatinge, 1975). While a large number of smooth muscle cells are likely to be involved, the response was radial not longitudinal. So any gap junctions that are present may determine the direction of current spread, and overall the orientation and gap junction coupling of the endothelium is ideally suited to conduct hyperpolarization along the mesenteric artery, presumably passing to the smooth muscle through functional myoendothelial gap junctions.

Limited spread of endothelial cell $[Ca^{2+}]_i$ changes

Our data show that a rise in endothelial cell $[Ca^{2+}]_i$ had little or no role in the spreading dilatation. While ACh stimulated a rise in endothelial cell $[Ca^{2+}]_i$ at the local site, no increase was observed 0.5 mm upstream of the stimulating pipette. This profile was also observed after focal stimulation with ACh in pressurized arterioles (Dora *et al.* 2003). So it appears that although Ca^{2+} and/or IP_3 can travel between cells, presumably though gap junctions, the rate and magnitude of intercellular coupling is too low to explain the dilatation. It was not possible to assess the potential intercellular Ca^{2+} signalling within 0.5 mm, as it is not possible to distinguish cells (approximately 150 μm long) that had been directly stimulated by ACh from those which had not. However, ACh clearly did not diffuse upstream to 0.5 mm. That a rise in endothelial cell $[Ca^{2+}]_i$ is not required for spreading hyperpolarization and dilatation at distances greater than 0.5 mm upstream, means that the EDHF response is not a prerequisite, as it does require an increase in endothelial cell $[Ca^{2+}]_i$ (Busse *et al.* 2002).

That levcromakalim was also able to stimulate spreading hyperpolarization and dilatation without a detectable rise in endothelial cell $[Ca^{2+}]_i$ supports this. It also follows that endothelial cell hyperpolarization *per se* does not drive a significant increase in endothelial cell $[Ca^{2+}]_i$. Hyperpolarizing or depolarizing voltage steps can increase or limit Ca^{2+} influx in endothelial cells in culture (Cannell & Sage, 1989; Schilling, 1989; Luckhoff & Busse, 1990*b*), although activation of K_{ATP} channels and associated hyperpolarization had little effect on $[Ca^{2+}]_i$ (Luckhoff & Busse, 1990*a*; Katnik & Adams, 1995). An inability of hyperpolarization to increase endothelial cell $[Ca^{2+}]_i$ has also

been reported in endothelial cells *in situ* in rat mesenteric arteries (Ghisdal & Morel, 2001), femoral arteries (Ohi *et al.* 2001), gracilis muscle arteries (Ungvari *et al.* 2002), and middle cerebral arteries (Marrelli *et al.* 2003). The latter observations are all consistent with our data.

Dye spread between cells in the mesenteric artery

The dye coupling experiments suggest that both homo- and heterocellular couplings are functional in the rat mesenteric arteries. The anatomical evidence for gap junctions between endothelial cells is extensive, and includes rat mesenteric arteries (Sandow & Hill, 2000; Gustafsson *et al.* 2003). However, the homocellular gap junctions between rat mesenteric artery smooth muscle cells are less readily observed, using either electron microscopy or immunohistochemical techniques (Hill *et al.* 2001; Gustafsson *et al.* 2003). In general, immunohistochemical images show a punctate distribution of connexins between smooth muscle cells, with no clear outlines of the cell wall, in marked contrast to endothelial cells in the same sections (Yeh *et al.* 1998). Further, it is not known whether these punctate structures occur at the end of cells, in a similar arrangement to the intercalated disks between cardiac myocytes (Beny & Connat, 1992), or along the sides of adjacent smooth muscle cells. In addition to homocellular gap junctions, definitive anatomical evidence for the existence of myoendothelial gap junctions is available from rat mesenteric arteries (Sandow & Hill, 2000; Gustafsson *et al.* 2003). The profile of dye coupling follows the anatomical evidence for gap junctions, as dye spread readily between the endothelial cells, but not so well between the smooth muscle cells. Also there was a small, but detectable, transfer of dye between endothelial and smooth muscle cells. The latter may relate to the low incidence of myoendothelial gap junctions, or to a low probability of heterocellular dye transfer even though connexons are present and can potentially pass current (Little *et al.* 1995; Emerson & Segal, 2000*a*,*b*; Yamamoto *et al.* 2001).

Overall, our data show that a resistance artery with 3–4 layers of smooth muscle can sustain a spreading vasodilatation with a very similar profile to that described in arterioles. Spread occurred independently of a change in cellular $[Ca^{2+}]$ and appeared to pass via the endothelium and not the smooth muscle layers.

References

Beny JL & Connat JL (1992). An electron-microscopic study of smooth muscle cell dye coupling in the pig coronary arteries. Role of gap junctions. *Circ Res* **70**, 49–55.

Busse R, Edwards G, Feletou M, Fleming I, Vanhoutte PM & Weston AH (2002). EDHF: bringing the concepts together. *Trends Pharmacol Sci* **23**, 374–380.

Busse R, Fichtner H, Luckhoff A & Kohlhardt M (1988). Hyperpolarization and increased free calcium in acetylcholine- stimulated endothelial cells. *Am J Physiol* **255**, H965–H969.

Cannell MB & Sage SO (1989). Bradykinin-evoked changes in cytosolic calcium and membrane currents in cultured bovine pulmonary artery endothelial cells. *J Physiol* **419**, 555–568.

Chen GF & Cheung DW (1997). Effect of K^+-channel blockers on ACh-induced hyperpolarization and relaxation in mesenteric arteries. *Am J Physiol* **272**, H2306–H2312.

Coats P & Hillier C (1999). Determination of an optimal axial-length tension for the study of isolated resistance arteries on a pressure myograph. *Exp Physiol* **84**, 1085–1094.

Crane GJ, Gallagher NT, Dora KA & Garland CJ (2003*a*). Small and intermediate calcium-dependent K^+ channels provide different facets of endothelium-dependent hyperpolarization in rat mesenteric artery. *J Physiol* **553**, 183–189.

Crane GJ, Walker SD, Dora KA & Garland CJ (2003*b*). Evidence for a differential cellular distribution of inward rectifier K channels in the rat isolated mesenteric artery. *J Vasc Res* **40**, 159–168.

Delashaw JB & Duling BR (1991). Heterogeneity in conducted arteriolar vasomotor response is agonist dependent. *Am J Physiol* **260**, H1276–H1282.

de Wit C, Roos F, Bolz SS, Kirchhoff S, Kruger O, Willecke K & Pohl U (2000). Impaired conduction of vasodilation along arterioles in connexin40-deficient mice. *Circ Res* **86**, 649–655.

Dora KA & Garland CJ (2001). Properties of smooth muscle hyperpolarization and relaxation to K^+ in the rat isolated mesenteric artery. *Am J Physiol* **280**, H2424–H2429.

Dora KA, Hinton JM, Walker SD & Garland CJ (2000). An indirect influence of phenylephrine on the release of endothelium-derived vasodilators in rat small mesenteric artery. *Br J Pharmacol* **129**, 381–387.

Dora KA, Xia J & Duling BR (2003). Endothelial cell signaling during conducted vasomotor responses. *Am J Physiol* **285**, H119–H126.

Doughty JM, Boyle JP & Langton PD (2000). Potassium does not mimic EDHF in rat mesenteric arteries. *Br J Pharmacol* **130**, 1174–1182.

Doyle MP & Duling BR (1997). Acetylcholine induces conducted vasodilation by nitric oxide-dependent and –independent mechanisms. *Am J Physiol* **272**, H1364–H1371.

Duling BR & Berne RM (1970). Propagated vasodilation in the microcirculation of the hamster cheek pouch. *Circ Res* **26**, 163–170.

Edwards G, Dora KA, Gardener MJ, Garland CJ & Weston AH (1998). K^+ is an endothelium-derived hyperpolarizing factor in rat arteries. *Nature* **396**, 269–272.

Emerson GG, Neild TO & Segal SS (2002). Conduction of hyperpolarization along hamster feed arteries: augmentation by acetylcholine. *Am J Physiol* **283**, H102–H109.

Emerson GG & Segal SS (2000*a*). Electrical coupling between endothelial cells and smooth muscle cells in hamster feed arteries: role in vasomotor control. *Circ Res* **87**, 474–479.

Emerson GG & Segal SS (2000*b*). Endothelial cell pathway for conduction of hyperpolarization and vasodilation along hamster feed artery. *Circ Res* **86**, 94–100.

Emerson GG & Segal SS (2001). Electrical activation of endothelium evokes vasodilation and hyperpolarization along hamster feed arteries. *Am J Physiol* **280**, H160–H167.

Figueroa XF, Paul DL, Simon AM, Goodenough DA, Day KH, Damon DN & Duling BR (2003). Central role of connexin40 in the propagation of electrically activated vasodilation in mouse cremasteric arterioles in vivo. *Circ Res* **92**, 793–800.

Fukao M, Hattori Y, Kanno M, Sakuma I & Kitabatake A (1997). Sources of Ca^{2+} in relation to generation of acetylcholine- induced endothelium-dependent hyperpolarization in rat mesenteric artery. *Br J Pharmacol* **120**, 1328–1334.

Garland CJ & McPherson GA (1992). Evidence that nitric oxide does not mediate the hyperpolarization and relaxation to acetylcholine in the rat small mesenteric artery. *Br J Pharmacol* **105**, 429–435.

Ghisdal P & Morel N (2001). Cellular target of voltage and calcium-dependent K+ channel blockers involved in EDHF-mediated responses in rat superior mesenteric artery. *Br J Pharmacol* **134**, 1021–1028.

Graham JM & Keatinge WR (1975). Responses of inner and outer muscle of the sheep carotid artery to injury. *J Physiol* **247**, 473–482.

Gustafsson F & Holstein-Rathlou N (1999). Conducted vasomotor responses in arterioles: characteristics, mechanisms and physiological significance. *Acta Physiol Scand* **167**, 11–21.

Gustafsson F, Mikkelsen HB, Arensbak B, Thuneberg L, Neve S, Jensen LJ & Holstein-Rathlou NH (2003). Expression of connexin 37, 40 and 43 in rat mesenteric arterioles and resistance arteries. *Histochem Cell Biol* **119**, 139–148.

Gustafsson H, Mulvany MJ & Nilsson H (1993). Rhythmic contractions of isolated small arteries from rat: Influence of the endothelium. *Acta Physiol Scand* **148**, 153–163.

Haas TL & Duling BR (1997). Morphology favors an endothelial cell pathway for longitudinal conduction within arterioles. *Microvasc Res* **53**, 113–120.

Hill CE, Phillips JK & Sandow SL (2001). Heterogeneous control of blood flow amongst different vascular beds. *Med Res Rev* **21**, 1–60.

Hilton SM (1959). A peripheral arterial conducting mechanism underlying dilatation of the femoral artery and concerned in functional vasodilatation in skeletal muscle. *J Physiol* **149**, 93–111.

Hinton JM & Langton PD (2003). Inhibition of EDHF by two new combinations of K^+-channel inhibitors in rat isolated mesenteric arteries. *Br J Pharmacol* **138**, 1031–1035.

Hirst GD & Neild TO (1978). An analysis of excitatory junctional potentials recorded from arterioles. *J Physiol* **280**, 87–104.

Katnik C & Adams DJ (1995). An ATP-sensitive potassium conductance in rabbit arterial endothelial cells. *J Physiol* **485**, 595–606.

Kurjiaka DT & Segal SS (1995). Conducted vasodilation elevates flow in arteriole networks of hamster striated muscle. *Am J Physiol* **269**, H1723–H1728.

Little TL, Xia J & Duling BR (1995). Dye tracers define differential endothelial and smooth muscle coupling patterns within the arteriolar wall. *Circ Res* **76**, 498–504.

Luckhoff A & Busse R (1990*a*). Activators of potassium channels enhance calcium influx into endothelial cells as a consequence of potassium currents. *Naunyn Schmiedebergs Arch Pharmacol* **342**, 94–99.

Luckhoff A & Busse R (1990*b*). Calcium influx into endothelial cells and formation of endothelium-derived relaxing factor is controlled by the membrane potential. *Pflugers Arch* **416**, 305–311.

Marrelli SP, Eckmann MS & Hunte MS (2003). Role of endothelial intermediate conductance KCa channels in cerebral EDHF-mediated dilations. *Am J Physiol* **285**, H1590–H1599.

Ohi Y, Takai N, Muraki K, Watanabe M & Imaizumi Y (2001). Ca2+-images of smooth muscle cells and endothelial cells in one confocal plane in femoral artery segments of the rat. *Jpn J Pharmacol* **86**, 106–113.

Oishi H, Budel S, Schuster A, Stergiopulos N, Meister J & Beny J (2001). Cytosolic-free calcium in smooth-muscle and endothelial cells in an intact arterial wall from rat mesenteric artery in vitro. *Cell Calcium* **30**, 261–267.

Oishi H, Schuster A, Lamboley M, Stergiopulos N, Meister JJ & Beny JL (2002). Role of membrane potential in vasomotion of isolated pressurized rat arteries. *Life Sci* **71**, 2239–2248.

Pohl U, Holtz J, Busse R & Bassenge E (1986). Crucial role of endothelium in the vasodilator response to increased flow in vivo. *Hypertension* **8**, 37–44.

Popp R, Brandes RP, Ott G, Busse R & Fleming I (2002). Dynamic modulation of interendothelial gap junctional communication by 11,12-epoxyeicosatrienoic acid. *Circ Res* **90**, 800–806.

Rivers RJ, Hein TW, Zhang C & Kuo L (2001). Activation of barium-sensitive inward rectifier potassium channels mediates remote dilation of coronary arterioles. *Circulation* **104**, 1749–1753.

Sandow SL & Hill CE (2000). Incidence of myoendothelial gap junctions in the proximal and distal mesenteric arteries of the rat is suggestive of a role in endothelium-derived hyperpolarizing factor–mediated responses. *Circ Res* **86**, 341–346.

Schilling WP (1989). Effect of membrane potential on cytosolic calcium of bovine aortic endothelial cells. *Am J Physiol* **257**, H778–H784.

Segal SS & Beny JL (1992). Intracellular recording and dye transfer in arterioles during blood flow control. *Am J Physiol* **263**, H1–H7.

Segal SS & Duling BR (1986). Flow control among microvessels coordinated by intercellular conduction. *Science* **234**, 868–870.

Tare M, Coleman HA & Parkington HC (2002). Glycyrrhetinic derivatives inhibit hyperpolarization in endothelial cells of guinea pig and rat arteries. *Am J Physiol* **282**, H335–H341.

Thorsgaard M, Lopez V, Buus NH & Simonsen U (2003). Different modulation by Ca^{2+}-activated K^+ channel blockers and herbimycin of acetylcholine- and flow-evoked vasodilatation in rat mesenteric small arteries. *Br J Pharmacol* **138**, 1562–1570.

Ungvari Z, Csiszar A & Koller A (2002). Increases in endothelial Ca(2+) activate K(Ca) channels and elicit EDHF-type arteriolar dilation via gap junctions. *Am J Physiol* **282**, H1760–H1767.

Walker SD, Dora KA, Ings NT, Crane GJ & Garland CJ (2001). Activation of endothelial cell IK_{Ca} and 1-ethyl-2-benzimidazolinone evokes smooth muscle hyperpolarization in rat isolated mesenteric artery. *Br J Pharmacol* **134**, 1548–1554.

Wesselman JPM, Schubert R, VanBavel E, Nilsson H & Mulvany MJ (1997). K_{Ca}-channel blockade prevents sustained pressure-induced depolarization in rat mesenteric small arteries. *Am J Physiol* **272**, H2241–H2249.

White R & Hiley CR (2000). Hyperpolarisation of rat mesenteric endothelial cells by ATP-sensitive K^+ channel openers. *Eur J Pharmacol* **397**, 279–290.

Yamamoto Y, Imaeda K & Suzuki H (1999). Endothelium-dependent hyperpolarization and intercellular electrical coupling in guinea-pig mesenteric arterioles. *J Physiol* **514**, 505–513.

Yamamoto Y, Klemm MF, Edwards FR & Suzuki H (2001). Intercellular electrical communication among smooth muscle and endothelial cells in guinea-pig mesenteric arterioles. *J Physiol* **535**, 181–195.

Yeh HI, Rothery S, Dupont E, Coppen SR & Severs NJ (1998). Individual gap junction plaques contain multiple connexins in arterial endothelium. *Circ Res* **83**, 1248–1263.

Acknowledgements

We are grateful for the helpful discussions and expertise provided by Dr Sergey Smirnov, and for the generous use of his equipment. This work was supported by the Wellcome Trust.